

Effect of Reverse Micelle Size on the Librational Band of Confined Water and Methanol

Dean S. Venables,[†] Kathie Huang, and Charles A. Schmuttenmaer*

Department of Chemistry, Yale University, 225 Prospect Street, P.O. Box 208107, New Haven, Connecticut 06520-8107

Received: March 29, 2001; In Final Form: May 29, 2001

We report measurement of the OH librational band in nanoscopic pools of water and methanol confined within reverse micelles. The librational band, which peaks near 670 cm^{-1} in the bulk liquids, shifts to lower frequency as the reverse micelle size decreases. In addition, the shape of the band changes considerably as a function of decreasing size. The librational band at all compositions is well fit by a two-state model based on the relative fractions of bound and free water (or methanol) within the reverse micelles.

Introduction

Reverse micelles are fascinating entities that have received much well-deserved attention. An important aspect of their behavior that has been overlooked, however, is the OH librational motion of hydrogen-bonding liquids confined to their interior. This band occurs near 670 cm^{-1} in bulk water and methanol and is very sensitive to the degree of hydrogen bonding.^{1–3} Liquids in confined spaces behave differently than their bulk counterparts, which is one of the reasons reverse micelles have been a subject of longstanding interest. Similarly, the effect of an interface on the properties of liquids has also stimulated much recent work. In addition to the fundamentally interesting chemical nature of these questions, the effect of size and interfacial interactions are also pertinent to other areas of science in which water is confined to nanoscopic environments.⁴ Such environments include biological molecules and membranes, porous rocks and clays, and zeolites.⁵ Confined environments may also be used to carry out a variety of reactions, either by modifying the properties of the encapsulated liquid or by bringing reactants into close contact.^{6,7} The focus of this study is to determine the effects of confinement upon the librational dynamics of hydrogen-bonding liquids.

The dimensions and shapes of reverse micelles are easily tunable, making them particularly useful for studying the effects of confinement on liquids. Their properties fall halfway between those of interfaces at solid surfaces and those of biological membranes. Reverse micelles typically consist of a spherical cavity of water (or some other polar liquid) surrounded by a shell of surfactant molecules that functions as an interface between the polar cavity and the nonpolar medium in which they are dispersed.⁸ The surfactant molecules orient themselves with their headgroup directed inward, making the interior interface ionic. Also, nonspherical reverse micelles can be obtained by using different surfactant molecules. For example, rodlike prolate spheroidal reverse micelles are formed when using sodium bis(2-ethylhexyl) phosphate (NaDEHP)⁹ and wormlike reverse micelles are obtained when using L- α -phosphatidylcholine (lecithin).¹⁰ Water-swollen solutions of AOT will result in formation of a bicontinuous microemulsion.^{9,11} Under the conditions used in this study, the reverse

micelles are spherical and quite monodisperse, and their size is manipulated easily and reproducibly by varying the ratio of molar concentrations of polar liquid to surfactant molecules, w_0 , where $w_0 = [\text{polar liquid}]/[\text{surfactant}]$.¹²

Water in reverse micelles has been extensively studied using a variety of techniques. Infrared spectroscopy,^{13–15} THz spectroscopy,¹⁶ NMR spectroscopy,^{17,18} Raman and inelastic light scattering,¹⁹ fluorescence upconversion,^{10,11,20,21} calorimetry,¹⁸ and molecular dynamics (MD) simulations^{8,22–25} have all been used to probe the properties of water within the micelles. A common finding of these studies is that the confined water molecules can be modeled either by a two- or three-state system.^{8,13,19} Water molecules confined within the micelles have thus been classified as either “bound” or “free” in the two-state models, while the three-state models also include “trapped” water molecules. In these descriptions, the free water is found at the center of the micelles and behaves like bulk water, bound water is found at the ionic layer of the micelles, and trapped water resides within the ionic layer.⁸ The fractions of bound and free water change relatively sharply with w_0 , so that by $w_0 = 10$ many of the properties of the confined liquid are rather similar to those of the bulk liquid.¹³

Considerably less work has been done on methanol-containing reverse micelles.^{11,21} It has been noted that methanol/AOT/isooctane reverse micelles are smaller than water/AOT/isooctane reverse micelles for a given value of w_0 , even though methanol is a larger molecule than water. Another difference is that a small amount of methanol is present in the isooctane solvent, whereas water is entirely confined within the interior of the reverse micelle.¹¹

We have investigated changes in the absorption band at 670 cm^{-1} that arise from librational motion of the hydrogen atom.^{1–3} This band is characterized by the motion of the OH group and is therefore a sensitive probe of the hydrogen-bonding environment. Although the OH stretch is also sensitive to the hydrogen-bonding environment of the molecule and has been extensively studied, the librational band and OH stretch respond differently to different environments. Compared to bulk water, for instance, weaker hydrogen bonding in the smallest micelles causes a 25% decrease in the librational frequency, whereas only a 3% increase is observed in the OH stretching frequency. The librational bands of hydrogen bonding and non-hydrogen-bonding molecules are better resolved than are the corresponding OH stretch bands of these states.

* Corresponding author. E-mail: charles.schmuttenmaer@yale.edu.

[†] Present address: National Metrology Laboratory, CSIR, P.O. Box 395, Pretoria 0001, South Africa.

A particular advantage of studying the librational band is that it corresponds to an *intermolecular*, and not *intramolecular*, motion. This allows spectra calculated from MD simulations of rigid molecules to be compared with experimental spectra for the first time. The comparison of simulation results to those determined from experiment is crucial for determining their accuracy. Once the simulations accurately represent quantities that are experimentally accessible, greater confidence can be placed in simulated properties that are not experimentally accessible. We have previously used a similar combination of experimental spectra of the librational band and MD simulations to investigate the effect of mixing in binary aqueous and methanolic mixtures.^{1–3}

In this study, we present the experimental spectra of water/AOT/isooctane and methanol/AOT/isooctane reverse micelles. Changes in the librational band of water and of methanol are investigated as a function of the size of the micelles. The observed shifts in the librational band are related to a two-state model based on bound and free water or methanol. Differences and similarities between water and methanol in the micelles are discussed.

Experimental Section

Reverse micelles were prepared with sodium bis(2-ethylhexyl) sulfosuccinate (also known as aerosol-OT, or AOT) from Fluka, isooctane from Aldrich, and either methanol from Mallinckrodt or deionized water. All substances were used as received. Samples were prepared on a mass basis by adding water or methanol to AOT to give w_0 values ranging from 1 to 40 for water-containing reverse micelles and 2 to 20 for methanol-containing reverse micelles. The samples were then diluted by the required mass (and volume) of isooctane to bring the AOT concentration to 0.060 mol/L. Other workers have noted that AOT contains about 0.15 molecules of residual water/AOT molecule.^{12,20,26} In keeping with other workers, this amount is considered negligible and ignored in the calculation of w_0 .

Infrared spectra of the samples in the region 400–1600 cm^{-1} were measured using a variable path length cell mounted in a standard Midac M1200 FTIR spectrometer that has been previously described.^{2,27} The temperature of the sample was about 24 °C. Spectra were recorded at 15 path lengths for each sample, and the Napierian power absorption coefficient of the sample, $\alpha(\omega)$, was calculated from Beer's Law:

$$\ln[I(\omega)/I_0(\omega)] = -\alpha(\omega)d, \text{ or upon rearrangement,} \\ \ln I(\omega) = -\alpha(\omega)d + \ln I_0(\omega) \quad (1)$$

Here $I(\omega)$ is the intensity of the transmitted light through path length d and $I_0(\omega)$ is the incident intensity. Path lengths in the range 0–2000 μm were used, depending on the absorbance of the sample, which in turn depends on the value of w_0 . We typically took data over a series of path lengths such that the transmitted intensity at 670 cm^{-1} was about 3% for the longest path lengths and about 85% for the shortest. This procedure gave a reasonably high signal-to-noise ratio while avoiding Etalon effects. The absorption coefficient can be precisely determined because partial reflections at interfaces do not vary as the path length is changed. Multiple measurements of the isooctane and AOT/isooctane spectra gave highly reproducible absorption coefficients, and measurements of the AOT/isooctane/water (or methanol) reverse micelle solutions had an uncertainty of less than 3%.

Our experimental objective is to determine the manner in which the librational band of the confined water or methanol

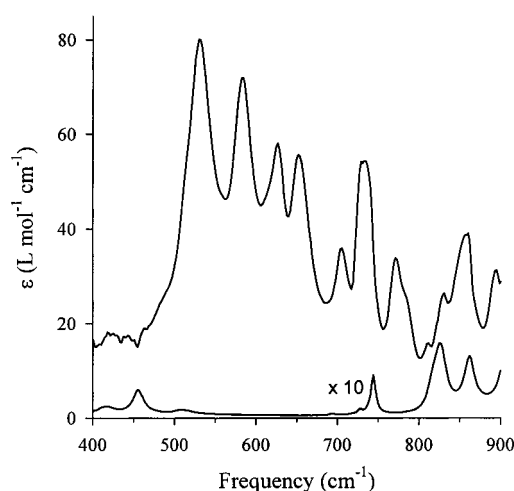


Figure 1. Molar extinction coefficient spectra for AOT (top curve) and isooctane ($\times 10$, bottom curve).

varies with micelle size. We do so by first determining the molar extinction coefficients of isooctane and AOT and then subtracting their contribution to the total sample absorption to yield the absorption of confined water or methanol.

The molar extinction coefficient of isooctane, $\epsilon_{\text{iso}}(\omega)$, is readily determined from the absorbance, $A = -\log[I(\omega)/I_0(\omega)]$, of a sample of neat isooctane using

$$\epsilon_{\text{iso}}(\omega) = \frac{A_{\text{iso}}(\omega)}{dc_{\text{iso}}} = \frac{\alpha_{\text{iso}}(\omega)}{2.303c_{\text{iso}}} \quad (2)$$

where c_{iso} is the isooctane concentration in mol/L. The molar extinction coefficient of AOT, $\epsilon_{\text{AOT}}(\omega)$, was calculated from the absorption coefficient of an AOT/isooctane sample, $\alpha_{\text{AOT/iso}}$, at 0.060 mol/L by subtracting the absorption arising from isooctane:

$$\epsilon_{\text{AOT}}(\omega) = \frac{\alpha_{\text{AOT/iso}}(\omega) - 2.303c_{\text{iso}}\epsilon_{\text{iso}}(\omega)}{2.303c_{\text{AOT}}} \quad (3)$$

The extinction coefficients of isooctane and AOT are shown in Figure 1. The molar extinction coefficients of water, $\epsilon_{\text{w}}(\omega)$, and methanol, $\epsilon_{\text{m}}(\omega)$, were similarly determined by subtracting the absorption due to isooctane and AOT:

$$\epsilon_{\text{w,m}}(\omega) = \frac{\alpha_{\text{AOT/iso/w,m}}(\omega) - 2.303[c_{\text{iso}}\epsilon_{\text{iso}}(\omega) + c_{\text{AOT}}\epsilon_{\text{AOT}}(\omega)]}{2.303c_{\text{w,m}}} \quad (4)$$

where $\alpha_{\text{AOT/iso/w}}$ is the absorption coefficient of the AOT/isooctane/water sample and $\alpha_{\text{AOT/iso/m}}$ is the absorption coefficient of the AOT/isooctane/methanol sample.

It has been suggested recently that the above straightforward analysis is not valid when applied to the far-infrared properties of water confined within reverse micelles.²⁸ This is because far-infrared measurements probe the dielectric relaxation of the confined water and are sensitive to the *collective* rotational diffusion, that is, delocalized modes. However, the librational band measured here arises from localized oscillatory modes involving only two or three molecules; it is not dielectric relaxation. We compared our approach to that of Hanai and co-workers, which includes contributions to the dielectric relaxation from the interfacial polarization of the AOT shell.^{29,30} We found that these two methods yielded the same results for

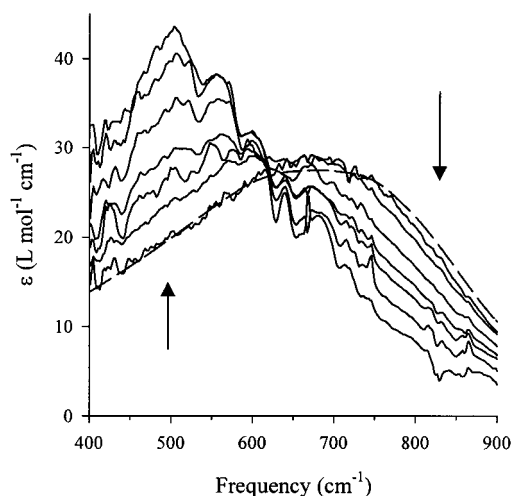


Figure 2. Molar extinction coefficient spectra of water confined within reverse micelles of various sizes. The progression of sizes from large to small w_0 values is indicated with the arrows. The arrows emphasize that the high-frequency portion of the spectrum decreases, while the low-frequency portion increases as a function of decreasing w_0 . Bulk water is shown with the smooth dashed curve,³¹ followed by reverse micelles with $w_0 = 40, 20, 10, 6, 4, 2,$ and 1.

the spectrum of the confined liquid. Therefore, we chose to use the more transparent treatment that is presented in eqs 1–4.

Results

A. Water. The molar extinction coefficient of water in reverse micelles of various sizes is shown in Figure 2. The absorption spectra of confined water molecules exhibit a large red shift as well as an increase in the magnitude of the molar extinction coefficient as w_0 decreases. The absorption band is red-shifted by about 170 cm^{-1} in the smallest micelles, which is a 25% decrease compared to the band maximum in bulk water at 670 cm^{-1} . The peak also becomes markedly more pointed with decreasing w_0 . The red-shifting and change in size of the absorption band indicates that the librational motion of water is strongly affected by confinement.

The librational band of water within the largest micelles ($w_0 = 40$) is essentially identical to that of bulk water,³¹ apart from a minor red shift. Therefore, one concludes that the librational motion of water molecules encapsulated in large reverse micelles ($\sim 12 \text{ nm}$ diameter) is almost identical to that in bulk water. The molar extinction coefficients determined for water at low w_0 values show small features that are correlated with the AOT spectrum, in addition to the large red shift. The confined water spectra show lower absorptions where the AOT spectrum has peaks, and vice versa, with the most prominent occurring at $540, 580, 630,$ and 660 cm^{-1} . These features are an artifact of the subtraction procedure and are most prominent in samples with small w_0 values, wherein AOT dominates the absorption spectrum. It is worth noting that these features are also present when carrying out the more complicated procedure described by Hanai and co-workers.^{29,30} The occurrence of these features suggests that the molar extinction coefficient of AOT at these frequencies is slightly smaller in the solvent-filled reverse micelles than in the empty micelles. We are most concerned with the general trends of the spectra and will not consider further these minor features.

The spectra show an isosbestic point near 620 cm^{-1} , suggesting a two-state system. Given our current signal-to-noise ratio and in the absence of direct evidence for a three-state system, we do not feel that a three-state model is justified for

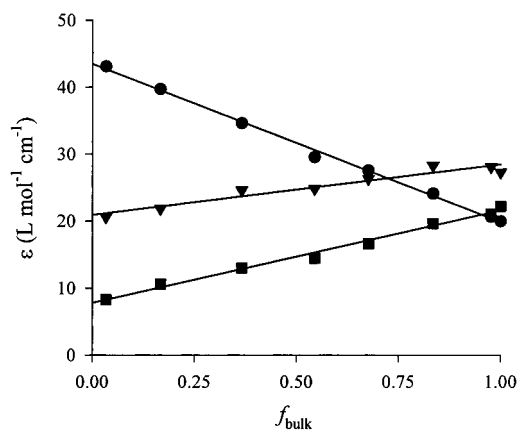


Figure 3. Typical frequency-dependent results of a global linear least-squares fit (solid lines) to the measured data at 500 cm^{-1} (circles), 650 cm^{-1} (triangles), and 800 cm^{-1} (squares).

our data. To assess how accurately the two-state model describes the librational motions, we have simultaneously incorporated all of the measured frequency-dependent molar extinction coefficients into a global fit. If the series of spectra indeed adhere to a two-state model, then the absorbance for a given frequency will vary linearly as a function of the fraction of bulk water, f_{bulk} , within the micelle for each value of w_0 . Unfortunately, the fraction f_{bulk} is not known a priori from the amount of water, AOT, and isoctane used to prepare the sample. Therefore, we perform a linear least-squares fit of the extinction coefficient for each frequency between 400 and 900 cm^{-1} as a function of f_{bulk} . The value of f_{bulk} for each value of w_0 is constrained to be the same at every frequency on a given iteration of the global fit. The difference between the measured spectra and the linear fits is then minimized by iteratively adjusting the values of f_{bulk} for the spectra taken at different values of w_0 . For bulk water, f_{bulk} is held fixed at 1.0 during the fitting procedure. Figure 3 shows representative cuts at $500, 650,$ and 800 cm^{-1} , where it is seen that the two-state model fits the data well. The results are shown in Figure 4 where the sizes shown from top to bottom are bulk water, followed by reverse micelles with $w_0 = 40, 20, 10, 6, 4, 2,$ and 1. Figure 5 plots f_{bulk} as a function of w_0 on the basis of these fits. The fraction of bulk water obtained by analyzing the OH stretching band for water/AOT/*n*-heptane reverse micelles³² is shown for comparison in Figure 5. The agreement between the two methods for $w_0 \geq 6$ is quite good. It is difficult to explain why the two methods disagree at small w_0 values, but it is surprising that D'Angelo et al. report that 40% of the water is bulklike at $w_0 = 2$.³² When $w_0 = 2$, the radius of the water pool is roughly 3 \AA ,¹² which would accommodate roughly 4 water molecules. It seems implausible that 1 to 2 of them behave like bulk water.

The spectra for pure bulk water and pure bound water resulting from the fit are the top and bottom traces, respectively, in Figure 4. The spectrum for pure bulk water is in good agreement with the experimental spectrum (shown as open squares). The spectrum of bound water is not experimentally measurable and is a result of the fit, hence the absence of open symbols. The fit assumes only a two-state model, and its validation rests in the level of agreement between the measured and calculated spectra. The spectra of pure bulk and pure bound water are summarized in Table 1. To extract the peak position, full width at half-maximum (fwhm), absorption maximum, and integrated absorption, Gaussian, and Lorentzian line shapes were fitted to the pure bulk and pure bound spectra, respectively. The integrated absorption is based on the fitted line shapes

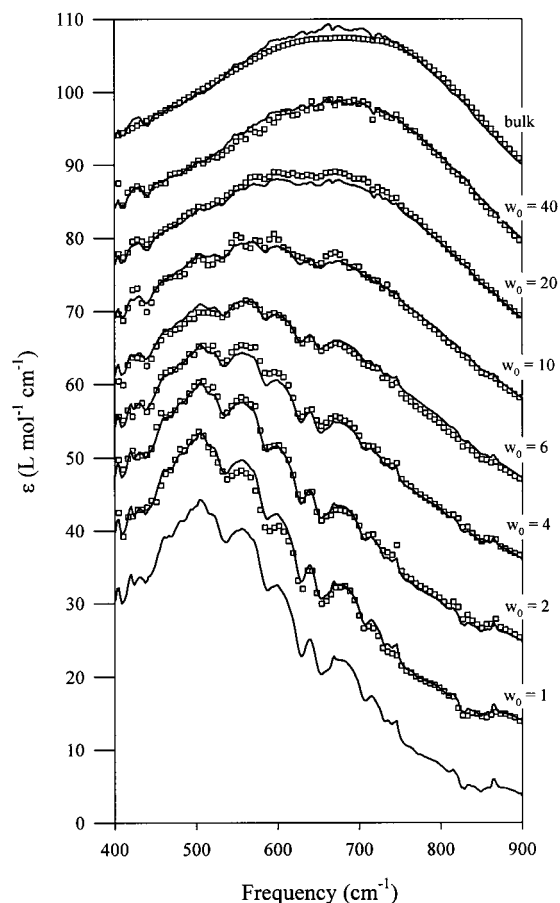


Figure 4. Results of a global linear least-squares fit of the measured water data. The fitted results are shown with solid lines, and the experimental data with open squares. The solid line not accompanied by symbols is the spectrum of pure bound water which results from the fit. For clarity, each spectrum is offset vertically by $10 \text{ L mol}^{-1} \text{ cm}^{-1}$.

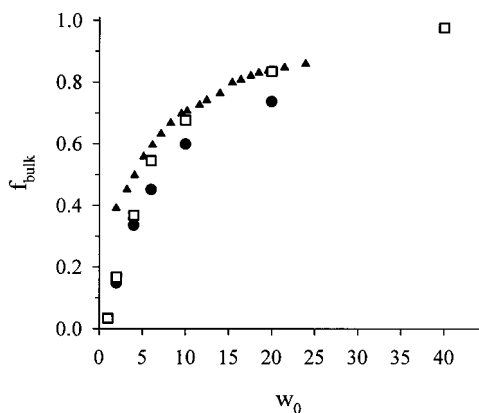


Figure 5. Fraction of bulk water (open squares) and bulk methanol (filled circles) as a function of w_0 . For comparison, the small filled triangles show the fraction of bulk water obtained by analyzing the OH stretching band for water/AOT/*n*-heptane reverse micelles.³² Note: D'Angelo et al. report w_{bound} rather than f_{bulk} , but the two are related through $w_{\text{bound}} = (1.0 - f_{\text{bulk}})w_0$.

because the experimental spectra are truncated at 400 and 900 cm^{-1} .

B. Methanol. The molar extinction coefficients of methanol in the reverse micelles are shown in Figure 6. The range of w_0 values studied was smaller than for water/AOT/isooctane because phase separation occurred for w_0 values greater than 20, and the spectra were unacceptably noisy for w_0 values less

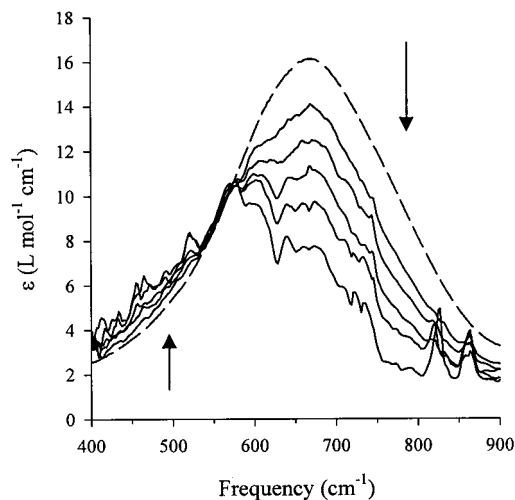


Figure 6. Molar extinction coefficient spectra of methanol confined within reverse micelles of various sizes. The progression of sizes from large to small w_0 values is indicated with the arrows. The arrows emphasize that the high-frequency portion of the spectrum decreases, while the low-frequency portion increases as a function of decreasing w_0 . Bulk methanol is shown with the smooth dashed curve,³³ followed by reverse micelles with $w_0 = 20, 10, 6, 4,$ and 2 .

TABLE 1: Parameters of OH Librational Band for the Pure Bulk and Pure Bound Spectra Determined from the Two-State Fit

| | peak posn (cm^{-1}) | fwhm (cm^{-1}) | peak max ($\text{L mol}^{-1} \text{ cm}^{-1}$) | integrated abs ($\text{L mol}^{-1} \text{ cm}^{-2}$) |
|----------------|-----------------------------------|------------------------------|---|---|
| bulk water | 660 | 465 | 27.8 | 13 700 |
| bound water | 510 | 301 | 42.6 | 17 400 |
| bulk methanol | 670 | 245 | 16.5 | 5 680 |
| bound methanol | 560 | 204 | 9.2 | 2 670 |

TABLE 2: Fraction of Methanol That Is Aggregated in Binary Methanol/Isooctane Mixtures

| methanol concn (M) | 0.03 | 0.06 | 0.12 | 0.3 | 1.6 |
|--------------------------|------|------|------|-----|------|
| fraction in clusters (%) | 0.0 | 0.0 | 16 | 52 | ~100 |

than 2. Unlike water, methanol is soluble in isooctane which presents additional complications. We determined the methanol concentration in a saturated binary methanol/isooctane mixture to be about 1.6 M (0.27 mole fraction). Measurements from 0.03 to 1.6 M showed that the librational band of binary methanol/isooctane mixtures does not shift and that its shape remains constant. It decreases in intensity at lower methanol concentrations because the relative fraction of methanol residing in clusters decreases as the concentration is reduced. The librational frequency of monomeric methanol dispersed in isooctane is very low due to the absence of hydrogen bonding and is outside the range of the spectrometer. Table 2 presents the fraction of aggregated methanol at various concentrations as obtained by comparing the relative height of the librational band to that for the C–O stretch, which is independent of the degree of aggregation because it is an intramolecular mode that does not participate in hydrogen bonding. The most important conclusion from studying binary methanol/isooctane mixtures is that the position of the librational band of methanol is constant. Thus, when the two-state model analysis is carried out, the bound fraction in the methanol/AOT/isooctane system can be confidently attributed to methanol confined within the reverse micelles. On the other hand, it is impossible to say whether the bulklike methanol is residing within the core or in the solvent, and the impact of this ambiguity is addressed in the Discussion.

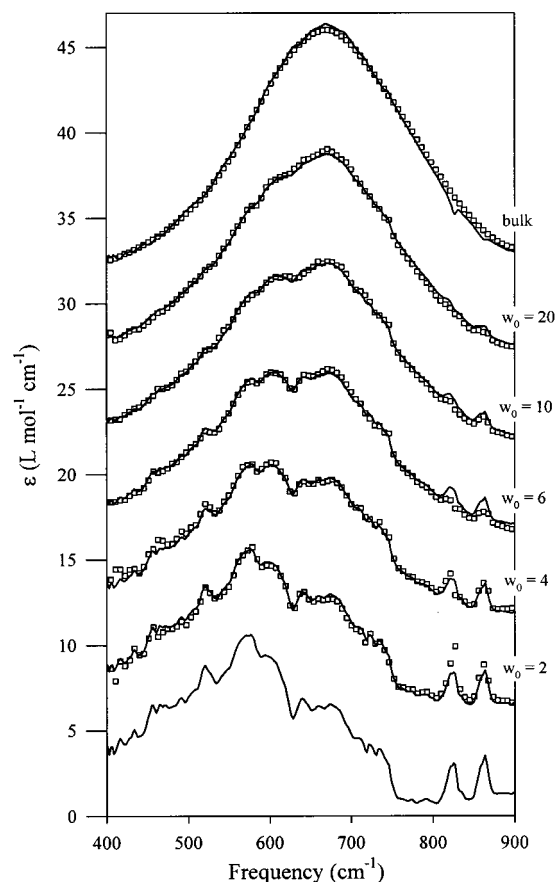


Figure 7. Results of a global linear least-squares fit of the measured methanol data. The fitted results are shown with solid lines, and the experimental data with open squares. The sizes shown from top to bottom are bulk methanol, followed by reverse micelles with $w_0 = 20, 10, 6, 4,$ and 2 . The solid line not accompanied by symbols is the spectrum of pure bound methanol which results from the fit. Each spectrum is offset vertically by $5 \text{ L mol}^{-1} \text{ cm}^{-1}$.

The maximum of the extinction coefficient for methanol in the largest micelle studied ($w_0 = 20$) is somewhat lower than that of bulk methanol³³ and is slightly red-shifted. Methanol confined in the large reverse micelles therefore does not seem to be completely bulklike, unlike water at $w_0 = 40$. This can be understood for two reasons: First, there is twice as much water relative to AOT compared to methanol for these two values of w_0 . Second, the interior of methanol-containing reverse micelles is significantly smaller than that for water for a given value of w_0 , even though methanol is a larger molecule than water. For example, when $w_0 = 10$, $r_{\text{water}} \approx 50 \text{ \AA}$ and $r_{\text{methanol}} \approx 23 \text{ \AA}$.¹¹

As the size of the reverse micelles decreases, the high-frequency portion of the methanol librational band decreases steadily and the lower frequency part of the band increases slightly. There is an isosbestic point in the molar extinction coefficient of methanol near 580 cm^{-1} . As in the case of water, the methanol spectra for small values of w_0 show artifacts due to absorption by AOT, as well as additional artifacts at $455, 827,$ and 861 cm^{-1} due to absorption by isooctane. The methanol data were also fit to a two-state model, and the results are shown in Figure 7. The values determined for f_{bulk} are plotted in Figure 5, and the spectra of pure bulk and pure bound methanol are summarized in Table 1.

C. SO_3^- Band. The SO_3^- symmetric stretch gives rise to an absorption band near 1050 cm^{-1} . Since SO_3^- is the AOT headgroup and is therefore found at the AOT/water interface,

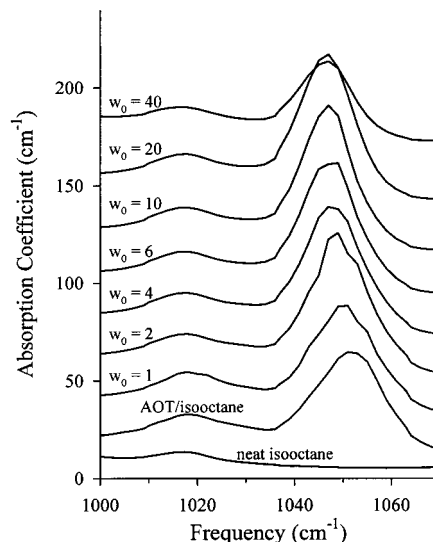


Figure 8. Absorption coefficient of SO_3^- symmetric stretch as a function of reverse micelle size. Neat isooctane is shown in the bottom trace, where a small feature at 1017 cm^{-1} is seen. Successive spectra have been offset by 20 cm^{-1} for clarity.

changes in this vibrational band reflect changes at the interface. There is only a single feature in the calculated gas-phase spectrum because all three oxygen atoms are equivalent, whereas we measure a smaller additional peak at 1018 cm^{-1} . As seen from the bottom spectrum in Figure 8, neat isooctane also has a peak at 1017 cm^{-1} which overlaps with this feature. However, careful inspection reveals that the isooctane peak is a factor of 2 smaller than the feature at 1018 cm^{-1} observed in the spectra of samples that contain AOT (all the other spectra in Figure 8). Furthermore, the AOT peak at 1018 cm^{-1} red-shifts as a function of w_0 value in the same manner as the primary peak at 1050 cm^{-1} . The fact that the peak has split into two peaks indicates that all three oxygen atoms are not equivalent in the condensed phase. The relative height of the two features is essentially independent of w_0 . In addition, the two largest water/AOT/isooctane reverse micelle sizes have a broad baseline absorption from water itself. The general trend observed that the band red-shifts slightly in going from $w_0 = 1$ to $w_0 = 40$ is in agreement with the findings of Li et al.⁹

The fact that the SO_3^- band is split, even when $w_0 = 0$, indicates that the degeneracy among the three oxygens is lifted in the condensed phase. The Na^+ counterion could preferentially form a weak complex with one of the oxygen atoms, causing it to become more negatively charged than the other two. The water molecules would then hydrogen bond to the remaining oxygens and the sodium ion.

A similar analysis for the methanol/AOT/isooctane reverse micelles could not be carried out. The C—O stretch in methanol occurs at 1030 cm^{-1} , which makes it difficult to observe the dependence of the SO_3^- band on micelle size. We attempted to subtract a shifted and rescaled bulk methanol spectrum from the measured data, but the resulting spectra depended tremendously on the amount of shift chosen. Therefore, it is currently not possible to state how strongly the SO_3^- band is affected by size in methanol-containing reverse micelles.

Discussion

The water and methanol spectra have qualitatively similar behavior as a function of reverse micelle size. Both water and methanol librational bands exhibit a significant red shift and become more pointed as the reverse micelle size becomes

smaller. The decrease in librational frequency, which is intimately related to the hydrogen-bonding environment, suggests that hydrogen bonds formed between water or methanol molecules are weaker in small cavities. The weaker hydrogen bonds in turn are probably a result of more strain in the hydrogen-bonding network within the cavity. The constraints imposed by the cavity size forces the associated structure, that is, the hydrogen bond network of water or methanol molecules, to adopt configurations that are no longer close to optimum. In water, the minimum energy configuration is an infinite 3-dimensional tetrahedral network, a configuration that cannot be maintained at the water–surfactant interface. Similarly, the 1-dimensional methanol chains that are a feature of bulk methanol will be forced to adopt relatively strained configurations. In both water and methanol the effect is probably more closely linked to strained hydrogen bond angles than to nonoptimal hydrogen bond lengths. Hartnig et al.³⁴ have observed the same effect in simulations of water in silica pores.

We attribute the larger red shift observed in water than in methanol to a relatively larger perturbation from the bulk environment. It is known that water is more affected by collective motions than is methanol.³⁵ Water has a much more narrowly defined minimum energy configuration, whereas chains of methanol molecules can more easily twist to accommodate the constraints imposed by the cavity. As the interior becomes smaller, the ability of methanol to form large prolate spheroids is inhibited and the chains will break up to form smaller prolate spheroids. The most likely position of the methanol molecules is in the middle of the chains, and their librational spectrum will not be highly dependent on the length of the chain. Since this motion is less influenced by the hydrogen-bonding network in the first place, the librational band will not shift as much. We have observed a similar effect in our experimental work on binary mixtures, where the red shift of the OH librational band is about 40 cm⁻¹ less in dilute methanol/acetonitrile mixtures than in dilute water/acetonitrile mixtures.^{1,2}

The changes in the magnitude of the extinction coefficients of water and methanol are more difficult to explain. Changes in the IR absorption are related to changes in the dipole derivative of the system. Therefore, an increase could be caused either by larger amplitude oscillations of individual molecules or by more concerted motions among molecules. One possibility would be to seek an explanation in the relative weakness of the hydrogen bonds in small micelles, which would allow water molecules to undergo larger amplitude librations and thereby result in the stronger IR absorption that is observed in water-containing micelles. Another explanation is suggested by the simulations of Ladanyi et al., which show that water molecules at the surfactant interface only donate one hydrogen bond to the surfactant headgroup.⁸ If this is the case, then the resultant single hydrogen bond donor water molecules should be able to librate more freely than if they donated two hydrogen bonds. The ability of the water molecules to move more freely would result in a larger oscillation of the molecular dipole and hence an increase in the molar extinction coefficient. This explanation would not apply to methanol because it can only donate a single hydrogen bond. It is also possible that motions of the water molecules become much more correlated when the size of the interacting cluster is smaller, which would also account for the increase in the molar extinction coefficient.

Trapped methanol is affected by the decreasing size in a different way. Methanol molecules that are hydrogen bonded to the headgroups of the surfactant molecules cannot donate

hydrogen bonds to other methanol molecules, and the methyl group would be directed toward the center of the reverse micelle, resulting in considerable steric congestion. Furthermore, it is known that methanol is soluble in isooctane, and it is possible that the size of the reverse micelle will affect the partitioning of the methanol between the reverse micelle core and the surrounding solvent. The methanol system should actually be described with a four-state model rather than a two-state model: there is bulklike and bound methanol within the reverse micelles, and there is bulklike and monomeric methanol residing in the solvent.

If the partitioning ratio of the methanol between the solvent and the reverse micelles was known, then the four-state model could be implemented (since the relative fractions of aggregated and monomeric methanol in the solvent is known from the methanol/isooctane binary mixtures). In any case, even though the partitioning ratio is not known, the values reported for f_{bulk} in Figure 5 are an upper limit. Furthermore, the loss of methanol to the solvent undoubtedly accounts for the majority of the decrease in integrated band intensity at smaller w_0 values.

Conclusions

The characteristics of the OH librational band of water and methanol confined within reverse micelles depend strongly on size. Both liquids exhibit a marked red shift as a function of size from the bulk to the smallest sized micelle. One notable difference between the water/AOT/isooctane and methanol/AOT/isooctane systems is that the peak value of the extinction coefficient increases in going to smaller sizes for water, while it decreases for methanol. The data over a large range of reverse micelle sizes for both systems are well described by a two-state model.

One of the goals of this work is to present experimental results that can be used for assessing the accuracy of MD simulations. There have been a number of computational studies of micelles,^{8,22–25} but the OH librational spectrum has yet to be reported. If the calculated spectra agree with the measured ones, then additional insight into the structure and dynamics of these systems could be obtained by analyzing the MD results in great detail. Dynamical quantities such as collective dipole spectra, single-dipole spectra, self- and cross-correlation terms, and linear and angular velocity spectra could all be determined. For example, if the single molecule spectra and collective dipole spectra are essentially indistinguishable, then collective contributions probably are not very important. Similarly, the self- and cross-terms will reveal the relative contributions of these two types of interactions and whether they enhance or oppose each other. The angular velocity autocorrelation spectra provide information about rotational motion about the x , y , and z axes that might not lead to a reorientation of the molecular dipole and, therefore, would not be experimentally accessible. In addition to dynamical quantities, structural information such as radial distribution functions at different positions within the reverse micelle, spatial distribution functions of molecules at different positions, and hydrogen-bonding information will also further our understanding of these system.

It should be noted, however, that simulations of reverse micelles present unique challenges compared to bulk liquid simulations. In particular, the parameters for describing the surfactant are largely unknown. Furthermore, a decision must be made as to how much detail to attribute to the surfactant. Ideally, the hydrophobic chains would be treated in atomic, or nearly atomic, detail, but that might make the computations prohibitively expensive, especially for large sizes. Existing

efforts could be continued by first calculating the librational spectra and comparing to the results presented here, which would show whether existing models are adequate.

Future work includes measuring the OH librational band for different reverse micelle systems that have spherical interiors, nonspherical rodlike interiors, nonspherical wormlike interiors, and bicontinuous media. This will separate the influence of the shape of the nanoscopic pool from that due to small dimensions. It will also be important to experimentally determine the partitioning ratio of methanol between the solvent and the reverse micelles to unambiguously determine f_{bulk} within the micelle. Molecular dynamics simulations will facilitate interpretation of the spectra, as well as the underlying causes for differences between methanol and water systems.

Acknowledgment. The authors thank the National Science Foundation for a CAREER award and the Sloan Foundation for partial support of this work.

References and Notes

- Venables, D. S.; Schmuttenmaer, C. A. *J. Chem. Phys.* **2000**, *113*, 11222–11236.
- Venables, D. S.; Chiu, A.; Schmuttenmaer, C. A. *J. Chem. Phys.* **2000**, *113*, 3243–3248.
- Venables, D. S.; Schmuttenmaer, C. A. *J. Chem. Phys.* **2000**, *113*, 3249–3260.
- Nandi, N.; Bhattacharyya, K.; Bagchi, B. *Chem. Rev.* **2000**, *100*, 2013–2045.
- Ricci, M. A.; Rovere, M. *J. Phys. IV* **2000**, *10*, 187–193.
- Menger, F. M.; Donohue, J. A.; Williams, R. F. *J. Am. Chem. Soc.* **1973**, *95*, 286–288.
- Menger, F. M.; Yamada, K. *J. Am. Chem. Soc.* **1979**, *101*, 6731–6734.
- Faeder, J.; Ladanyi, B. M. *J. Phys. Chem. B* **2000**, *104*, 1033–1046.
- Li, Q.; Weng, S. F.; Wu, J. G.; Zhou, N. F. *J. Phys. Chem. B* **1998**, *102*, 3168–3174.
- Willard, D. M.; Levinger, N. E. *J. Phys. Chem. B* **2000**, *104*, 11075–11080.
- Riter, R. E.; Kimmel, J. R.; Undiks, E. P.; Levinger, N. E. *J. Phys. Chem. B* **1997**, *101*, 8292–8297.
- Zulauf, M.; Eicke, H. F. *J. Phys. Chem.* **1979**, *83*, 480–486.
- Onori, G.; Santucci, A. *J. Phys. Chem.* **1993**, *97*, 5430–5434.
- Temsamani, M. B.; Maeck, M.; El Hassani, I.; Hurwitz, H. D. *J. Phys. Chem. B* **1998**, *102*, 3335–3340.
- Jain, T. K.; Varshney, M.; Maitra, A. *J. Phys. Chem.* **1989**, *93*, 7409–7416.
- Mittleman, D. M.; Nuss, M. C.; Colvin, V. L. *Chem. Phys. Lett.* **1997**, *275*, 332–338.
- Maitra, A. *J. Phys. Chem.* **1984**, *88*, 5122–5125.
- Hauser, H.; Haering, G.; Pande, A.; Luisi, P. L. *J. Phys. Chem.* **1989**, *93*, 7869–7876.
- D'Aprano, A.; Lizzio, A.; Liveri, V. T.; Aliotta, F.; Vasi, C.; Migliardo, P. *J. Phys. Chem.* **1988**, *92*, 4436–4439.
- Riter, R. E.; Willard, D. M.; Levinger, N. E. *J. Phys. Chem. B* **1998**, *102*, 2705–2714.
- Shirota, H.; Horie, K. *J. Phys. Chem. B* **1999**, *103*, 1437–1443.
- Laaksonen, L.; Rosenholm, J. B. *Chem. Phys. Lett.* **1993**, *216*, 429–434.
- Brown, D.; Clarke, J. H. R. *J. Phys. Chem.* **1988**, *92*, 2881–2888.
- Tobias, D. J.; Klein, M. L. *J. Phys. Chem.* **1996**, *100*, 6637–6648.
- Simonson, T. *Chem. Phys. Lett.* **1996**, *250*, 450–454.
- D'Angelo, M.; Onori, G.; Santucci, A. *Nuovo Cimento Soc. Ital. Fis., D* **1994**, *16*, 1601–1611.
- Venables, D. S. *Spectroscopy and Molecular Dynamics Simulations of Aqueous and Nonaqueous Mixtures*; Yale University: New Haven, CT, 2000.
- Mittleman, D. M. Personal communication.
- Hanai, T.; Imakita, T.; Koizumi, N. *Colloid and Polym. Sci.* **1982**, *260*, 1029–1034.
- Zhang, H. Z.; Sekine, K.; Hanai, T.; Koizumi, N. *Colloid and Polym. Sci.* **1983**, *261*, 381–389.
- Bertie, J. E.; Lan, Z. D. *Appl. Spectrosc.* **1996**, *50*, 1047–1057.
- D'Angelo, M.; Onori, G.; Santucci, A. *J. Phys. Chem.* **1994**, *98*, 3189–3193.
- Bertie, J. E.; Zhang, S. L. *J. Chem. Phys.* **1994**, *101*, 8364–8379.
- Hartnig, C.; Witschel, W.; Spohr, E.; Gallo, P.; Ricci, A.; Rovere, M. *J. Mol. Liq.* **2000**, *85*, 127–137.
- Ladanyi, B. M.; Skaf, M. S. *J. Phys. Chem.* **1996**, *100*, 1368–1380.